Interaction of yeast eIF4G with spliceosome components Implications in pre-mRNA processing events

RESEARCH PAPER

RNA Biology 6:5, 563-574; November/December 2009; © 2009 Landes Bioscience

Interaction of yeast eIF4G with spliceosome components

Implications in pre-mRNA processing events

Panagiota Kafasla,[1,3,*] J. David Barrass,[1] Elizabeth Thompson,[1] Micheline Fromont-Racine,[2] Alain Jacquier[2] Jean D. Beggs[1] and Joe Lewis[1,†]

[1]Wellcome Trust Centre for Cell Biology; University of Edinburgh; Edinburgh, UK; [2]Genetique des Interactions Macromoleculaires; Institut Pasteur (CNRS-URA2171); Paris, France; [3]Department of Biochemistry; University of Cambridge; Cambridge, UK

[†]Current address: Chemical Biology Core Facility; EMBL; Heidelberg, Germany

Key words: pre-mRNA processing, spliceosome, eIF4G, Prp11p, Snu71p

As evidenced from mammalian cells the eukaryotic translation initiation factor eIF4G has a putative role in nuclear RNA metabolism. Here we investigate whether this role is conserved in the yeast *Saccharomyces cerevisiae*. Using a combination of in vitro and in vivo methods, we show that, similar to mammalian eIF4G, yeast eIF4G homologues, Tif4631p and Tif4632p, are present both in the nucleus and the cytoplasm. We show that both eIF4G proteins interact efficiently in vitro with UsnRNP components of the splicing machinery. More specifically, Tif4631p and Tif4632p interact efficiently with U1 snRNA in vitro. In addition, Tif4631p and Tif4632p associate with protein components of the splicing machinery, namely Snu71p and Prp11p. To further delineate these interactions, we map the regions of Tif4631p and Tif4632p that are important for the interaction with Prp11p and Snu71p and we show that addition of these regions to splicing reactions in vitro has a dominant inhibitory effect. The observed interactions implicate eIF4G in aspects of pre-mRNA processing. In support of this hypothesis, deletion of one of the eIF4G isoforms results in accumulation of un-spliced precursors for a number of endogenous genes, in vivo. In conclusion these observations are suggestive of the involvement of yeast eIF4G in pre-mRNA metabolism.

Introduction

The cap (m^7GpppN) structure added co-transcriptionally to RNA polymerase II transcripts has been shown to influence many aspects of RNA metabolism, including pre-mRNA splicing,[1,2] 3' end formation,[3] export from the nucleus,[4-6] stability[7] and translation.[8] In the nucleus, the cap structure interacts with the predominantly nuclear cap-binding complex (CBC), a heterodimer consisting of cap-binding proteins CBP20 (Mud13p in *S. cerevisiae*) and CBP80 (Sto1p or Gcr3p in *S. cerevisiae*).[9,10] CBP20 is highly conserved from yeast to human, whereas CBP80 is far less conserved. CBP20 recognizes and binds capped RNA in conjunction with CBP80.[11] CBC plays a direct role in precursor messenger RNA (pre-mRNA) splicing, promoting the association of U1 small nuclear ribonucleoprotein particle (snRNP) with the cap-proximal 5' splice site.[2,12] In *Saccharomyces cerevisiae*, CBC interacts with Snu56p, a yeast-specific component of the U1 snRNP and a *cbp20*-Δ *cbp80*-Δ double mutant strain shows synthetic lethality with *SNU71*, a gene encoding for another component of the yeast U1 snRNP, Snu71p.[13] Furthermore, CBC exits from the nucleus to the cytoplasm together with the mRNA,[4-6] where it is thought to be replaced by the eIF4F complex.

In the cytoplasm, the effect of the cap structure on mRNA translation is mediated by a trimeric complex termed eukaryotic translation initiation factor 4F, eIF4F. eIF4F consists of the cap-binding subunit eIF4E, eIF4G and the RNA-helicase eIF4A.[14] eIF4G acts as a bridge between the cap structure and components of the ribosomal initiation complex.[14,15] In addition to eIF4E and eIF4A, eIF4G interacts with the poly(A)-binding protein PABP (Pab1p in yeast) facilitating the functional association of the 3' end of an mRNA with its 5' end to promote translation,[16] while the association between eIF4G and eIF4E markedly enhances the binding of the latter to the cap structure.[14] eIF4G and CBP80 are both characterized by the presence of the MIF4G domain, a structural motif known to be present in many proteins involved in RNA metabolism.[17,18] In *S. cerevisiae* there are two functionally redundant in translation isoforms of eIF4G, encoded by the genes *TIF4631* and *TIF4632*.[19]

A stable association of eIF4G with CBC detected in the nucleus of human cells plays possibly a role in coupling RNA-processing events in the nucleus with mRNA translation in the cytoplasm.[20] In mammalian cells, the interaction between eIF4G and CBC is required for the "pioneering" round of translation that leads to nonsense mediated decay (NMD). NMD is a

*Correspondence to: Panagiota Kafasla; Email: pk303@cam.ac.uk
Submitted: 06/01/09; Revised: 08/10/09; Accepted: 08/18/09
Previously published online: www.landesbioscience.com/journals/rnabiology/article/9861

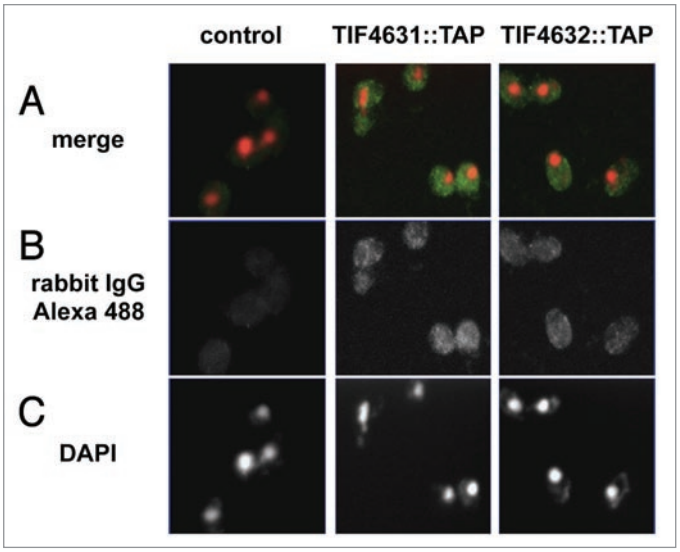

Figure 1. Yeast eIF4G homologues are distributed between the nucleus and the cytoplasm. Wild-type yeast cells (control) and cells expressing TIF4631:TAP or TIF4632:TAP were grown to OD_{600}: 0.2–0.4 and immobilized on slides as described in Materials and Methods. The location of Tif4631p and Tif4632p was detected with rabbit IgG Alexa 488 labeled (B). DAPI staining was used for the localization of the nuclei (C). The merged image is also presented in (A).

surveillance mechanism comprising the recognition and subsequent degradation of mRNAs bearing a premature termination codon.[21] Research in human cell lines suggests that both nuclear and cytoplasmic NMD occur on CBC-associated rather than eIF4E-associated mRNA, suggesting a role for CBC in translation.[22,23] In mammalian cells, NMD is translation and splicing dependent.[24-27] Ferraiulo et al.[28] reported that translation initiation factor eIF4AIII, a mammalian nucleo-cytoplasmic shuttling protein that interacts physically or functionally with eIF4G, is loaded onto the mRNA during splicing in the nucleus and then functions during NMD, indicating one more link between nuclear and cytoplasmic RNA processing events.

In *Saccharomyces cerevisiae* the domain of eIF4G responsible for the interaction with CBC resides between the eIF4E binding motif and the MIF4G domain.[29] Fortes et al.[29] proposed a role for the CBC-eIF4G interaction in the exchange of CBC for eIF4E and/or the direct recruitment of nascent mRNA for translation. However, it is not known whether this interaction occurs in the cytoplasm or in the nucleus. The latter can not be excluded since CBC as well as many components of the translation machinery are present in both cellular compartments.[4,30-32] In *S. cerevisiae* the interaction between eIF4G and CBC is not required for the first round of mRNA translation that proceeds NMD, while the exact role of this interaction is yet to be defined.[33] Yeast two-hybrid experiments have previously suggested that *S. cerevisiae* splicing factors, such as Prp11p and Snu71p could interact with the yeast eIF4G protein,[34] and the interaction of Prp11p with Tif4631p was proposed by Ho et al.[35] in a high throughput mass spectrometric protein complex identification screen. In human cells, association of eIF4G with pre-mRNA and the spliceosome, as well as partial co-localization of nuclear eIF4G with spliceosomal snRNPs are suggestive of a role for eIF4G in nuclear RNA-processing, perhaps in coupling splicing to other nuclear events and to translation.[20]

In the present work we assess the role of yeast eIF4G proteins in processing of RNA in the nucleus. We show the presence of eIF4G in the yeast nucleus and identify nuclear components that interact with eIF4G. We characterize in detail the interaction of eIF4G with protein and RNA components of the yeast spliceosome. We further investigate the possible role of yeast eIF4G in pre-mRNA splicing in vitro, and we show that depletion of one of the eIF4G homologues in vivo results in accumulation of intron containing pre-mRNAs for a number of endogenous genes. Our results suggest that yeast eIF4G has a role in pre-mRNA processing in the nucleus.

Results

Subcellular localization of Tif4631p and Tif4632p. To determine whether the yeast homologues of eIF4G, Tif4631p and Tif4632p, are present in both the cytoplasm and the nucleus, similarly to their human homologues, the proteins were expressed from their native promoter as C-terminally TAP-tagged fusion proteins and their localization was determined by indirect fluorescence and confocal microscopy. Both Tif4631p-TAP and Tif4632p-TAP were, as expected, found to be abundant in the cytoplasm (**Fig. 1A and B**). In addition, TAP-tagged Tif4631p and to a lesser extent Tif4632p could be both detected also in the nucleus, as shown in **Figure 1B**, in comparison to **C** where the location of the nuclei is indicated, and in the merged image **A**. This finding prompted us to determine whether the yeast eIF4G homologues can interact with components of the splicing machinery, similar to the situation observed in human extracts.[20]

Interaction of Tif4631p and Tif4632p with spliceosomal snRNPs. Whole cell extracts were made from strains expressing either Tif4631p-TAP or Tif4632p-TAP and the tagged proteins were precipitated using protein A Sepharose. An isogenic wild type strain was used as a negative control. Co-precipitated RNAs were purified, resolved on a denaturing gel, analysed by northern blot analysis with oligonucleotide probes specific to U1, U2, U4, U5 and U6 snRNAs (**Fig. 2A**) and the efficiency of precipitation was quantified (see legend of **Fig. 2B**). The eIF4G homologues reproducibly pulled down U1 snRNA. More specifically, ~20% of the input levels of U1 snRNA were pulled down by Tif4631p-TAP, whereas ~6% was precipitated by Tif4632-TAP (**Fig. 2A and B**), while more than 60% of the input U1 snRNA levels were precipitated under the same conditions by the TAP-tagged yeast CBP20 homologue, Mud13p (data not shown). The interaction of Tif4631p with U1 snRNA was reduced to ~10% of the input levels in increased salt concentration, whereas the less efficient interaction of this particular UsnRNA with Tif4632p could withstand salt much better, remaining at similar levels at 350 mM NaCl (**Fig. 2A and B**). Furthermore, ~7% of the input levels of U6 snRNA and ~10% of U4 snRNA were also pulled down by both eIF4G homologues, however these amounts were significantly reduced by increased salt concentration, mainly for Tif4631p and to a lesser extent for Tif4632p (**Fig. 2B**). Finally,

less than 5% of the input levels of U5 and U2 snRNAs were precipitated by the eIF4G homologues, and these interactions were greatly abolished when salt was increased to 350 mM NaCl (**Fig. 2B**). There was no significant precipitation of UsnRNAs from whole cell extracts prepared from the isogenic wild type strain (**Fig. 2A**, lanes 2 and 3) indicating that the detected RNAs were pulled down via their interaction with Tif4631-TAP and Tif4632-TAP proteins. These results suggest a specific interaction of both Tif4631p and Tif4632p mainly with U1 snRNA, with the interaction of Tif4631p and U1snRNA being more prominent (**Fig. 2**). In addition, both proteins can pull down to a similar extent U4 and U6 snRNAs (**Fig. 2B**).

Interaction of Tif4631p and Tif4632p with protein components of U1 and U2 snRNPs. There is evidence from yeast 2-hybrid screens that Tif4631p can interact specifically with the U2 snRNP protein, Prp11p and the U1 snRNP specific protein Snu71p, whereas Tif4632p was found to interact with Prp11p.[34] To assess these interactions GST-Prp11p and GST-Snu71p fusion proteins were expressed in *E. coli* and bound to Glutathione-Sepharose beads. The immobilized proteins were incubated with ^{35}S-labeled Tif4631p or Tif4632p and the purified complexes were analysed by SDS-PAGE and fluorography. Both Tif4631p and Tif4632p were pulled down by the immobilized GST-Prp11p very efficiently (**Fig. 3A**, lanes 1 and 2). Both proteins were also pulled down by GST-Snu71p, although in substantially lower amounts than with GST-Prp11p (**Fig. 3A**, lanes 7 and 8), whereas no protein was bound to Glutathione-Sepharose beads alone (lanes 4–6), indicating that the observed binding was specific. Incubation of the immobilized GST-Prp11p with ^{35}S labelled Snu71p and analysis of the purified complexes gave no detectable signal (**Fig. 3A**, lane 3), showing that the interaction detected between Tif4631p, Tif4632p and GST-Prp11p and -Snu71p is specific. We propose that there is a specific association between Prp11p and Tif4631p, characterized by the presence of two pools of complexes, since a great percentage of the interaction was lost at increased salt concentration

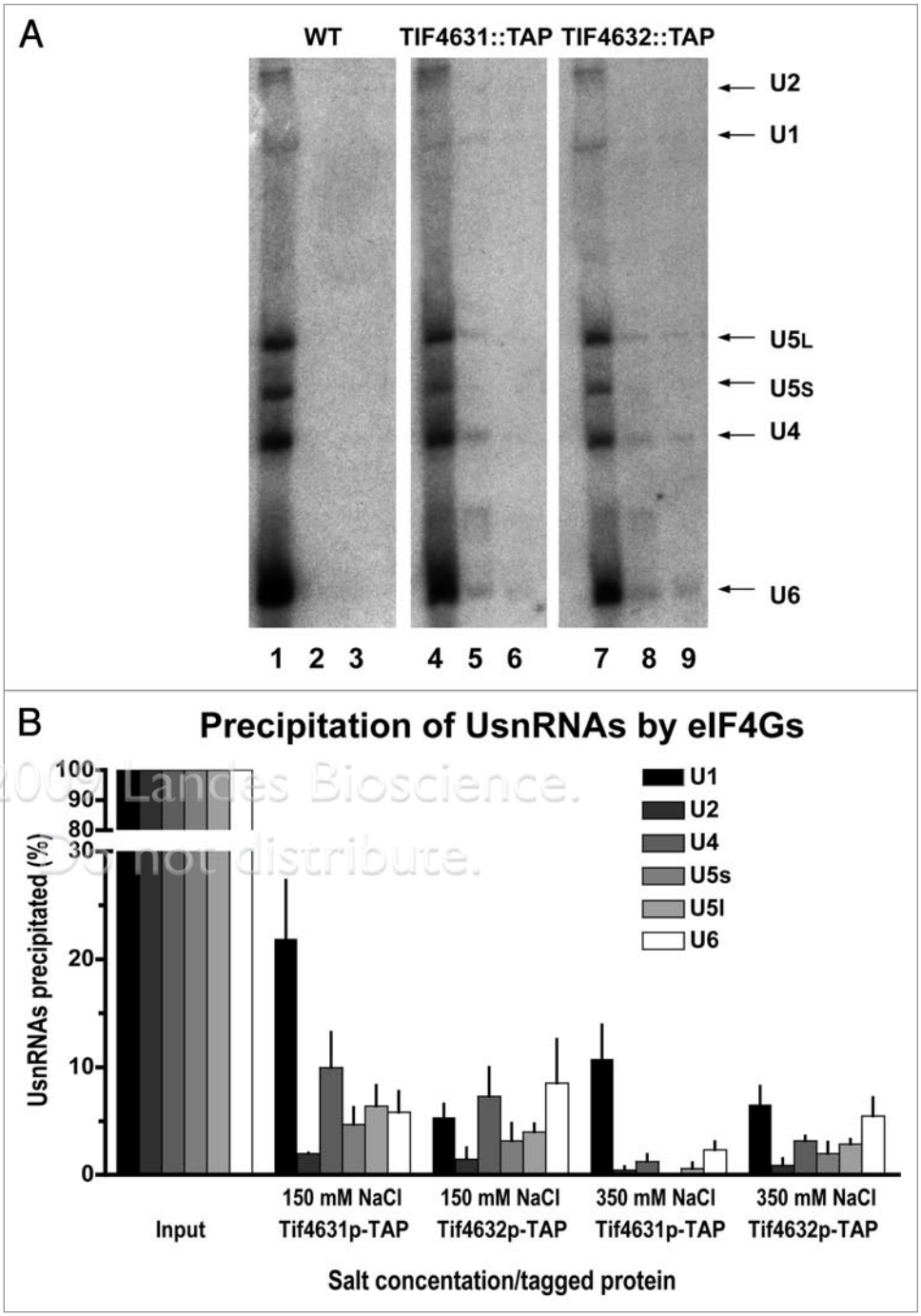

Figure 2. Yeast eIF4G homologues can precipitate U1 and U2 snRNA in vitro. (A) Yeast extracts derived from strains expressing either Tif4631p-TAP (lanes 4–6) or Tif4632p-TAP (lanes 7–9), as well as the isogenic wild-type strain (lanes 1–3), were incubated with IgG-Sepharose beads under increasing salt concentration (lanes 2, 5, 8: 150 mM NaCl, lanes 3, 6, 9: 350 mM NaCl). The co-precipitated RNAs, as well as 20% of the input RNAs (lanes 1, 4, 7), were assayed by northern blotting, using specific oligonucleotide-probes for each of the U1, U2, U4, U5 and U6 snRNAs. (B) Densitometry and Phosphorimager analysis were both used to quantify the signal produced by the northern analysis presented in (A), using the TotaLab software (Nonlinear Dynamics, UK) and ImageQuant software respectively. The results presented are means ± SEM from three independent experiments.

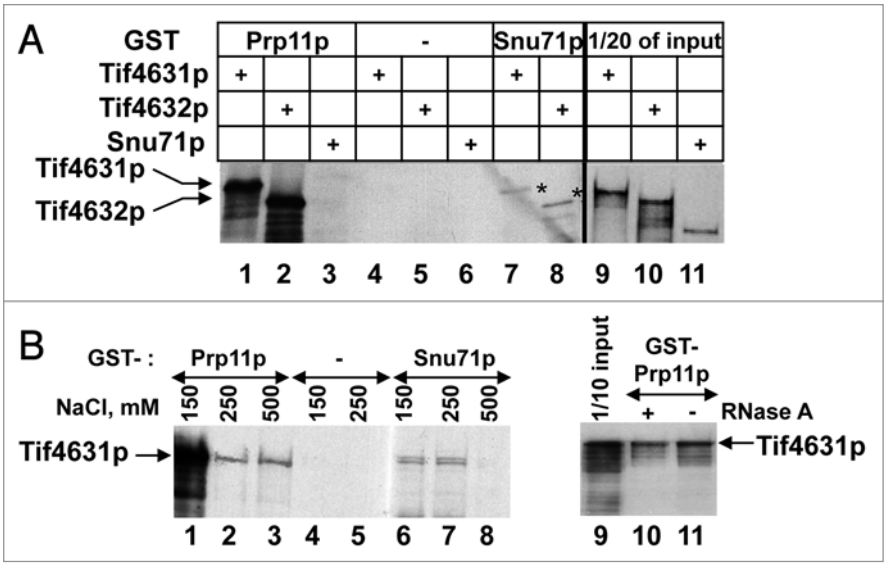

Figure 3. Yeast eIF4G homologues interact with protein components of U1 and U2 snRNPs. (A) Immobilized GST-Prp11p (lanes 1–3) or GST-Snu71p (lanes 7 and 8) were incubated with ^{35}S-labeled Tif4631p, Tif4632p or Snu71p as described in Materials and Methods. The pulled-down proteins were resolved by SDS-PAGE, and visualized by autoradiography. GST alone immobilized on Glutathione-Sepharose beads was used as negative control (lanes 4–6). 1/20 of input ^{35}S-labeled proteins were also analysed (lanes 9–11). (B) Immobilized GST-Prp11p (lanes 1–3, 10 and 11) or GST-Snu71p (lanes 6–8) or GST alone (lanes 4 and 5) were incubated with ^{35}S-labeled Tif4631p, in the presence of increasing amounts of NaCl, or in the presence (+) or absence (-) of 200 ng/ml RNase A as indicated. The pulled-down proteins were resolved by SDS-PAGE, and visualized by autoradiography. 1/10 of the input ^{35}S-labeled proteins were also analysed (lane 9).

(up to 500 mM NaCl, **Fig. 3B**, lanes 1–3) while a small but significant percentage was persistent even at very high salt concentration. The interaction of Tif4631p with Snu71p was less resistant to the highest salt concentration used (**Fig. 3B**, lanes 6–8). RNase A treatment did not significantly alter the binding pattern, demonstrating that the interaction of Tif4631p and Tif4632p with both Prp11p and Snu71p is not RNA mediated (**Fig. 3B**, lanes 9–11, and data not shown).

Mapping of the domain of Tif4631p that interacts with splicing factors. To map the domains of Tif4631p that are responsible for the interactions with both Snu71p and Prp11p, N-terminal and C-terminal truncated forms of Tif4631p were generated, in vitro translated and used in GST pull down experiments using immobilized GST-Prp11p or GST-Snu71p (**Fig. 4A**). Deletion of residues 657–952 from the C-terminus of Tif4631p had no effect on binding efficiency of this protein to either GST-Prp11p or GST-Snu71p. Further deletion of amino acids 593–656 resulted in about 30% less efficient binding, whereas complete loss of pull-down efficiency was evidenced when amino acids 267–592 were also deleted (**Fig. 4A**). In addition, deleting the N-terminal residues up to amino acid 452 did not affect the binding efficiency of Tif4631p for either Prp11p or Snu71p (**Fig. 4A**). Further deletion of amino acids 453–493 resulted in approximately 50% reduction of the interaction efficiency with Prp11p, while still maintaining the interaction with Snu71p (**Fig. 4A**). After sequential deletion of amino acids 494–528 the truncated Tif4631p could not be pulled down by GST-Prp11p, whereas deletions extending beyond amino acid 567 resulted in loss of interaction with GST-Snu71p (**Fig. 4A**). The above suggest that the minimal region of Tif4631p required for interaction with Prp11p resides between residues 494 and 529 (**Fig. 4A**).

To define in further detail the minimal domain of Tif4631p required for interaction with Prp11p, 10aa deletion mutants of Tif4631p were expressed and assayed in pull down assays with GST-Prp11p as described above. **Figure 4B** shows that individual deletion of aa 491–501, 534–544 or 566–576 reduced significantly the amount of Tif4631p mutant that could be pulled down by GST-Prp11p (lanes 2–4, compared to lane 1), suggesting that these residues contribute to the interaction between these proteins. It is noteworthy that none of these deletions was enough to abolish the interaction completely. In addition, substitution of residues 496–498 or 506–508 with Ala residues showed that these specific amino acids, and more crucially residues 506–508 are important for the interaction of Tif4631p with GST-Prp11p (**Fig. 4B**, lanes 6, 7 compared to lane 1). On the other hand, deletion of residues 457–467, 469–479 (**Fig. 4C**, lane 5 and data not shown), as well as 565–647 (**Fig. 4C**) did not affect significantly the levels of Tif4631p mutant that could be pulled down by GST-Prp11p, as expected (**Fig. 4A**). Taken together these findings suggest that the absolutely essential region of Tif4631p required for the interaction with Prp11p resides between amino acids 508–529. It is obvious, however, that all amino acids within the region of 494–529 contribute to the high affinity interaction of Tif4631p with Prp11p, since deletion of individual domains within this region, in the context of an otherwise full-length protein do not abolish the interaction completely. The fact that a Tif4631p mutant lacking aa 504 to 952 can not be pulled down by GST-Prp11p (**Fig. 4C**) and neither can be a mutant lacking residues 1–529 (**Fig. 4A**), verifies that residues 504–529 are absolutely required for the interaction of Tif4631p with GST-Prp11p in our pull down assays. Using the same approach we mapped the region of Tif4631p interacting with Snu71p between amino acids 567 and 647 (**Fig. 4A**) and that was verified by the finding that deletion of residues 565–647 of Tif4631p resulted in loss of the interaction of this protein with GST-Snu71p in our pull-down assays (**Fig. 4D**, lane 4).

Fortes et al.[29] found that amino acids 490–592 are required for the interaction of Tif4631p with yeast CBC. The fact that this region includes also the residues necessary for interaction with Prp11p and Snu71p, as described above, prompted us to investigate whether we could characterize in more detail the individual interactions of this domain. Using our Tif4631p truncated and deletion mutants we found that deletion of amino acids 491–501 resulted in more than 30% reduction of the interaction

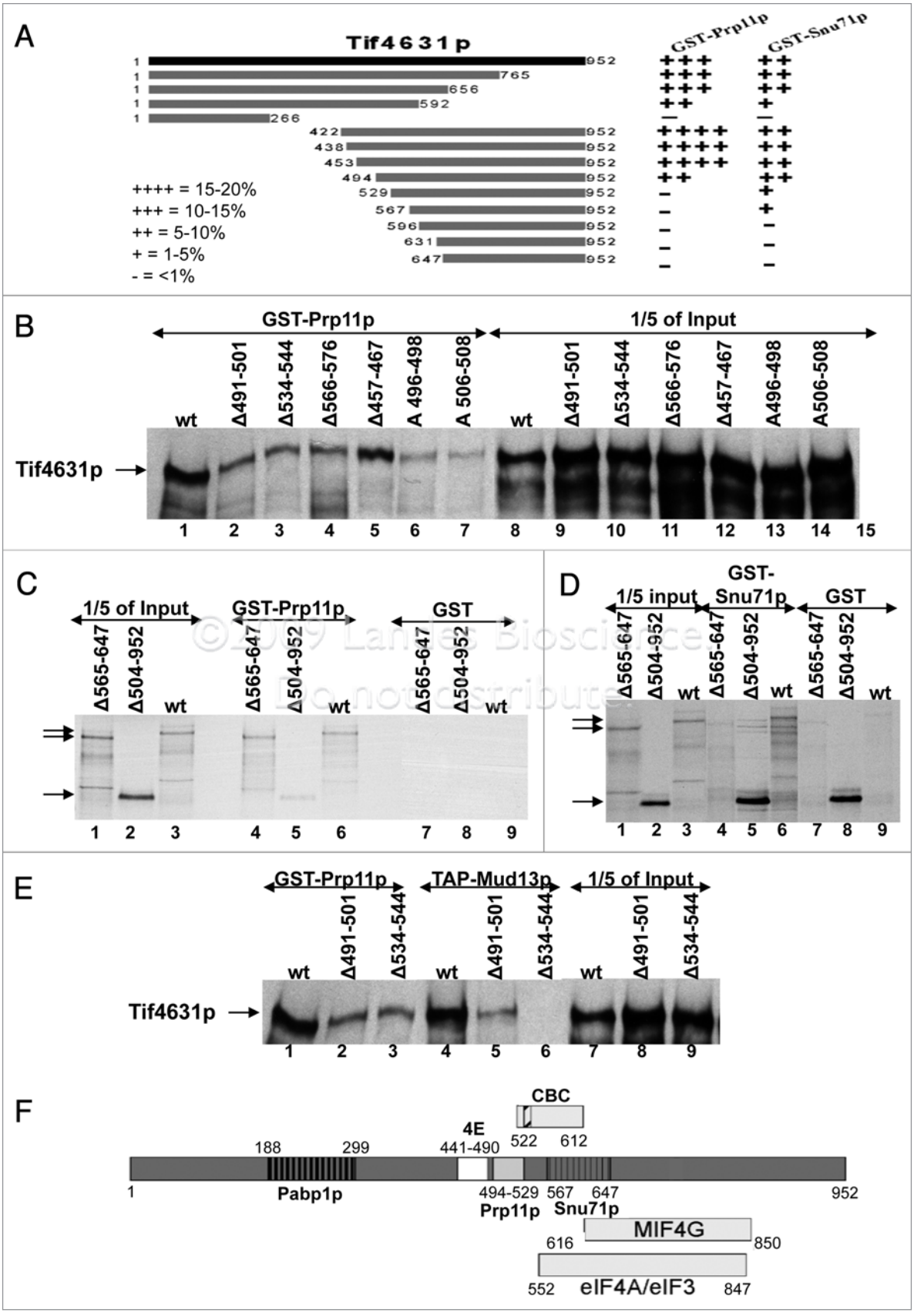

Figure 4. For figure legend, see page 568.

Figure 4. Detailed mapping of the interaction of Tif4631p with Snu71p and Prp11p. (A) Schematic representation of the deletion mutants of Tif4631p. Pull-down experiments were performed by incubation of immobilized GST-Pp11p or GST-Snu71p with ^{35}S-labeled full-length or truncated Tif4631p mutants and analysed as described in Figure 3A. Densitometry was used to quantify the respective autoradiographs and the quantification results are presented as % percentages of the input protein used for the pull-down experiments. (B) Immobilized GST-Prp11p (lanes 1–7) was incubated with ^{35}S-labeled Tif4631p (wt) or the Tif4632p-mutant proteins indicated, as described in Figure 3. The pulled-down proteins were resolved by SDS-PAGE, and visualized by autoradiography. 1/5 of input ^{35}S-labeled proteins were also analysed (lanes 8–15). (C) Immobilized GST-Prp11p (lanes 4–6) was incubated with ^{35}S-labeled Tif4631p (wt) or the Tif4632p mutants indicated. The pulled-down proteins were resolved by SDS-PAGE, and visualized by autoradiography. GST alone immobilized on Glutathione-Sepharose beads was used as negative control (lanes 7–9). 1/5 of input ^{35}S-labeled proteins were also analysed (lanes 1–3). The full length ^{35}S-labeled proteins are indicated by arrows. (D) Immobilized GST-Snu71p (lanes 4–6) were incubated with ^{35}S-labeled Tif4631p (wt) or the Tif4632p mutants indicated. The pulled-down proteins were resolved by SDS-PAGE, and visualized by autoradiography. GST alone immobilized on Glutathione-Sepharose beads was used as negative control (lanes 7–9). 1/5 of input ^{35}S-labeled proteins were also analysed (lanes 1–3). The full length ^{35}S-labeled proteins are indicated by arrows. (E) Immobilized GST-Prp11p (lanes 1–3) or TAP-Mud13p (lanes 4–6) were incubated with ^{35}S-labeled wild-type Tif4631p (wt) or Tif4631p mutants lacking amino acid residues 491–501 (Δ491-501), or 534–544 (Δ534-544). The pulled-down proteins were resolved by SDS-PAGE and visualized by autoradiography. 1/5 of the input ^{35}S-labeled proteins was also analysed for comparison. (F) Schematic representation of the domain of Tif4631p required for interaction with Prp11p, Snu71p and CBC. Other characterized domains of Tif4631p are also indicated (see text for details).

efficiency with TAP-Mud13p (**Fig. 4E**, lanes 4 and 5) and we identified the minimal region of Tif4631p required for interaction with TAP-tagged yeast CBP20 (Mud13p) in vitro to reside between residues 522 and 612 (data not shown). In addition, we identified a Tif4631p deletion mutant lacking amino acids 534–544, that could still bind to GST-Prp11p, but had abolished completely the interaction with TAP-Mud13p (**Fig. 4E**, lanes 3 and 6). This finding indicates that residues 534–544 of Tif4631p are essential for the interaction with yeast CBC. More importantly, the fact that Tif4631p-Δ(534-544) interacts with Prp11p but not with Mud13p shows that Tif4631p can interact with Prp11p in a CBC-independent manner. A summary of the above described domains, as well as a schematic representation of the domains of Tif4631p that are known to be required for interaction with Pabp1p[36] and eIF4E,[37] as well as the MIF4G domain[17] are shown for comparison in **Figure 4E**.

Sequence comparison shows that the region of Tif4631p that interacts with Prp11p, Snu71p and Mud13p is also very highly conserved in Tif4632p.[19] Using the same method as for Tif4631p, N-terminal and C-terminal truncation mutants of Tif4632p were assayed for their efficiency to bind to Prp11p and Snu71p and amino acids 424–609 were defined as the minimum region of Tif4632p required for interaction with Prp11p and Snu71p (data not shown).

Inhibition of splicing in vitro by Tif4631p/Tif4632p interaction domains. As shown in **Figure 3C**, the binding of $Tif4631_{494\text{-}952}$ to Prp11p was noticeably less than that observed with $Tif4631_{453\text{-}952}$. To obtain the minimum domain of Tif4631p that interacts efficiently with U1 and U2 snRNP proteins we constructed a Tif4631p domain mutant spanning amino acids 453 to 647, so as to include the region of Tif4631p that interacts with Snu71p. We refer to this construct as "Tif4631p(453-647)". Similarly, a construct with the Tif4632p domain required for interaction with both Prp11p and Snu71p was made and we refer to this construct as "Tif4632p(424-609)". After verifying, by pull-down experiments with GST-Prp11p and GST-Snu71 proteins, that domains Tif4631p(453-647) and Tif4632p(424-609) interact specifically with both Prp11p and Snu71p in vitro (data not shown), we used these constructs to determine whether Tif4631p(453-647) and Tif4632p(424-609) can influence splicing by supplementing in vitro splicing reactions with increasing amounts of these conserved domains fused to GST at their N-terminus. Addition of either GST-Tif4631p(453-647) (**Fig. 5A**, lanes 3–5) or GST-Tif4632p(424-609) (lanes 6–8) resulted in inhibition of splicing, as judged by the production of less intermediate (intron-3' exon) and final (intron-lariat) products of splicing, compared to the control (**Fig. 5A**, lane 2). Addition of GST alone had a minor effect in the efficiency of the splicing reaction (**Fig. 5A**, lanes 9–11). Consequently, addition of increasing amounts of either the Tif4631p or the Tif4632p domains in the splicing reaction resulted in an increasing inhibitory effect (**Fig. 5B**). Addition of the GST-Tif4631p mutant lacking amino acids 534–544, and therefore unable to interact with yeast CBP20, in in vitro splicing reaction showed that this dominant negative effect could not be attributed to selective sequestration of CBC by Tif4631p (data not shown). The above findings suggest that inhibition of splicing caused by Tif4631p(453-647) and Tif4632p(424-609) is possibly due to sequestration of spliceosomal components like Prp11p and Snu71p away from the spliceosomal machinery.

Deletion of TIF4631 results in accumulation of certain pre-mRNAs in vivo. The interaction of Tif4631p and Tif4632p with components of U1 and U2 snRNPs, together with the ability of Tif4631p(453-647) and Tif4632p(424-609) domains to inhibit splicing in vitro, suggested a possible role for the yeast eIF4G homologues in splicing. To test this hypothesis, given that double deletion of the yeast eIF4G homologues is lethal,[19] we assayed splicing in vitro using extract prepared from a strain deleted of TIF4631, and expressing TAP-tagged Tif4632p that could sequentially be depleted by IgG-Sepharose beads. Analysis of the RNA products of splicing showed no significant difference in the levels of splicing between control and TIF4631 deleted/Tif4632p depleted extracts, indicating that Tif4631p or Tif4632p could not be made limiting for efficient splicing in vitro. Western blot analysis performed to check the depletion level of Tif4632p in the extracts showed that we could not completely deplete Tif4632p. Consequently, we can not completely exclude the possibility that Tif4631p and Tif4632p play a role in splicing, since we possibly could not reduce yeast eIF4G homologues to limiting levels for splicing in vitro. We therefore focused our attention on splicing in vivo by assaying the splicing efficiency of different pre-mRNAs globally in the wild type and *tif4631*-Δ strains using

splicing microarrays.[38] Total RNA was extracted from the above strains and hybridized to slides containing an array of oligonucleotides able to hybridize to all the intron-containing RNAs of *S. cerevisiae* and to distinguish between pre-mRNAs and mRNAs.[38] These oligonucleotides were complementary to the 5' exon-intron junction of each one of the *S. cerevisiae* pre-mRNAs, or to the intron itself or to the exon-exon junction of each one of the mature mRNAs (**Fig. 6A**). For data normalization purposes oligonucleotides able to hybridize to the 3' exon of each one of all the pre-mRNAs and mRNAs were also used.

Out of 257 genes tested, there were 6 that consistently, in five independent experiments, showed accumulation of pre-mRNA at least two-fold or more in the *tif4631*-Δ strain compared to the isogenic control strain (**Table 2**). Similar analysis performed for a *tif4632*-Δ strain did not show any significant change in the pre-mRNA or mRNA levels, compared to the isogenic control strain. The microarray results were then verified for the gene YJR145C, for which accumulation of pre-mRNA could be detected in the *tif4631*-Δ strain compared to the wt strain, using primer extension experiments (**Fig. 6B**, lanes 1 and 2; quantified in **C**). As a positive control we used the *prp2-1* strain, that is deficient in splicing and exhibits a much stronger splicing block at the non-permissive temperature (37°C)[14] (**Figs. 6B**, lanes 3 and 4 and **5C**). YJR145C is the systematic name used for the gene *RPS4A*, which gives rise to the ribosomal protein Rps4Ap, a protein identical to Rps4Bp. The primer used for the primer extension experiment could hybridize to pre-mRNA and mRNA entities representing both genes. A two- to three-fold accumulation of the pre-mRNAs corresponding to both *RPS4A* and *RPS4B* could be detected in the *tif46321*-Δ strain compared to the isogenic control strain, whereas strain *prp2-1* showed the expected strong splicing deficient phenotype (**Fig. 6C**).

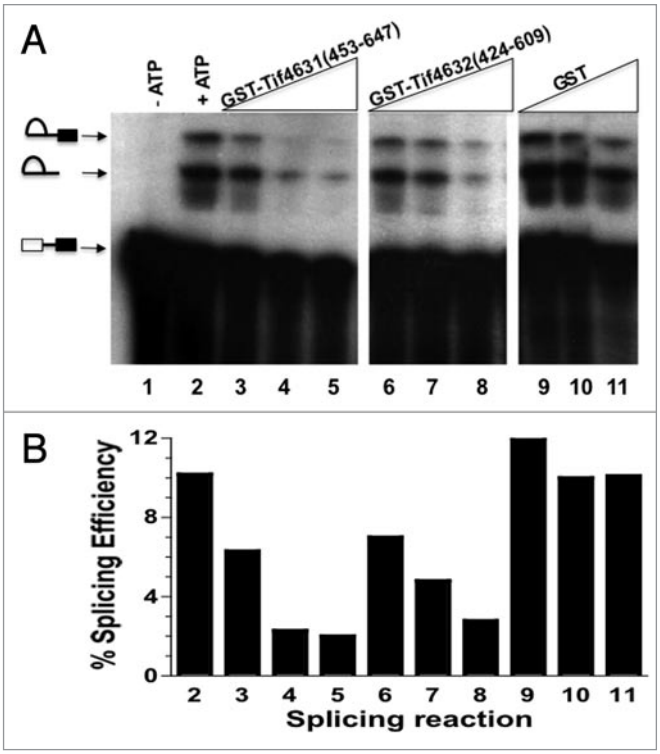

Figure 5. Tif4631p(453-647) and Tif4632p(424-609) inhibit splicing in vitro. (A) Increasing amounts (0.2–1 μg) of a GST-Tif4631p(453-647) (lanes 3–5) or GST-Tif4632p(424-609) (lanes 6–8) or GST alone (lanes 9–11), were added to in vitro splicing reactions, and the RNA products were analyzed by denaturing gel electrophoresis and autoradiography. Lane 1 shows the pre-mRNA used and lane 2 shows the control reaction without the addition of any protein. (B) Histogram derived from the quantification of data presented in (A) by phosphorimager analysis. Both spliced products (lariat and lariat exon) were quantified and are represented as a percentage of the unspliced pre-mRNA.

Discussion

In the present study, we investigate the putative role of the yeast translation initiation factor eIF4G in nuclear pre-mRNA processing. Using in situ localization we show that, in addition to their expected cytoplasmic localization, eIF4G homologues of *S. cerevisiae*, Tif4631p and to a smaller extent Tif4632p, exhibit a significant presence in the yeast nucleus. This agrees with previous reports that have demonstrated the presence of eIF4G in the nucleus of HeLa cells, indicative of a possible role for eIF4G in nuclear RNA processing.[20,39] Huh et al.[40] however, report that both yeast eIF4G homologues are located in the cytoplasm, using C-terminally GFP-tagged fusion constructs, fluorescent microscopy and an experimental approach different to ours.

In the cytoplasm, eIF4G plays an essential role in translation by acting as an adapter molecule during the initiation phase of protein synthesis. Within its sequence it contains domains that interact with eIF4E, eIF4A, eIF3, PABP and Mnk1.[14] In addition, *S. cerevisiae* eIF4G has been shown to interact with the cap binding complex, CBC, via a domain between eIF4E and eIF3 binding sites.[29] McKendrick et al.[20] have shown that, in mammalian cells, a nuclear pool of eIF4G is closely associated with CBC. Moreover, it is known that CBC in the nucleus promotes association of U1 snRNA with the cap proximal 5' splice site.[2,12]

Consistent with these results, we provide evidence here for the interaction of yeast eIF4G homologues with spliceosomal UsnRNPs. We show that mainly Tif4631p, and Tif4632p to a lesser extent, interact with U1 snRNA. In addition, both eIF4G homologues are also shown to interact stably with the U1 snRNP component Snu71p, either directly or via other proteins present in the reticulocyte lysate used in our assays. This particular interaction, however, is much less efficient possibly because Snu71p alone does not mediate the interaction of eIF4G proteins with U1 snRNP. Using pull-down binding assays, we show that both eIF4G homologues interact very efficiently and stably with Prp11p, a U2 snRNP component in an RNA-independent manner, whereas our TAP-tagged eIF4G homologues can only pull down a minor amount of U2 snRNA in vitro. This finding suggests that the high affinity interaction of yeast eIF4G proteins with Prp11p is independent of its interaction with U2 snRNA. The finding that eIF4G homologues can pull down U4 and U6 snRNAs to a similar extent is not unexpected since the existence of a penta-snRNP complex has been proposed for yeast.[41]

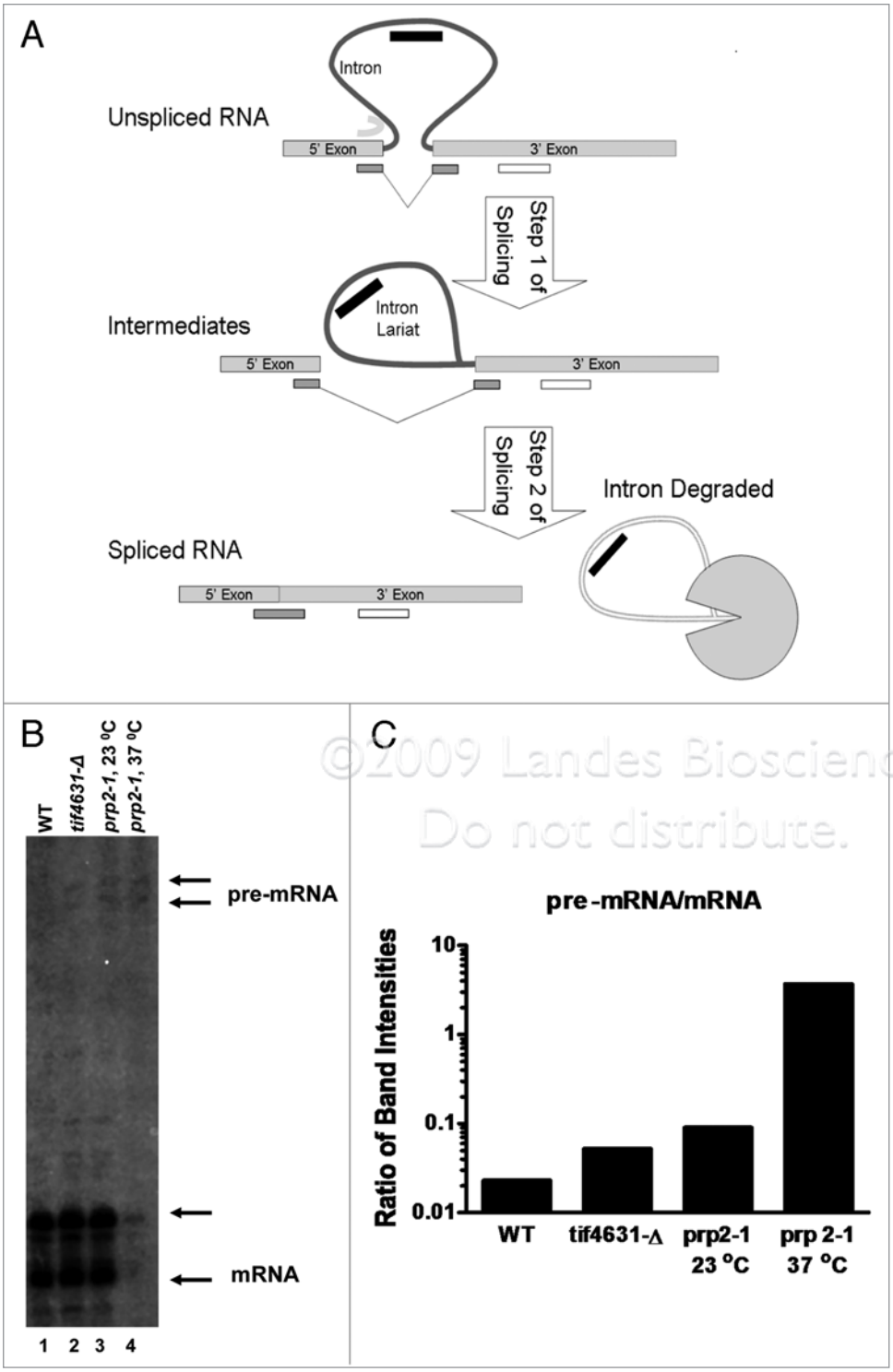

Figure 6. Accumulation of pre-mRNAs in *tif4631-Δ* strain in vivo. (A) Schematic overview of the splicing microarray. Four different probes able to detect intermediate species of the two stages of splicing were designed and used on the microarray. The intron probe (black), as well as the 5'-exon-intron probe (dark grey) can only be hybridized to by un-spliced RNA. The mature junction probe (grey) will only be hybridized to by processed mRNA, whereas the exon 2 probe (white) will be hybridized to by both pre-mRNA and mRNA and is used as a control to remove effects due to differential gene expression. (B) Total RNA was extracted from the *tif4631-Δ* strain as well as from the isogenic wild-type and was used in primer extension experiment, as described in Materials and Methods. The cDNAs were analysed by denaturing gel electrophoresis and autoradiography. RNA from strain *prp2-1*, grown either at 23°C or at 37°C was also used in the same experiment as a control. The positions of both the mature and precursor mRNAs for both *RPS4A* and *RPS4B* are indicated. (C) Quantification of the bands corresponding to both pre-mRNAs and mRNAs of the gel presented in (B) by phosphorimaging.

Fine mapping of the individual domains of eIF4G proteins required for the interaction with Prp11p, CBC and Snu71p shows that they are distinct, but adjacent to each other and together they form an "interaction domain" that resides in a region that is highly conserved between the two yeast eIF4G isoforms. Addition of a recombinant form of the above defined "interaction domain" of yeast eIF4G can efficiently inhibit splicing in vitro, possibly by interacting with spliceosomal components and sequestering them away from the splicing machinery, supporting the hypothesis that eIF4G proteins can participate in pre-mRNA processing events.

To further investigate the possible role of yeast eIF4G in splicing, we undertook a global analysis of pre-mRNA splicing using microarrays. A subset of six pre-mRNAs showed a reproducible two- to three-fold accumulation of pre-mRNAs in strains deleted of the *TIF4631* compared to the isogenic control (**Table 2**). Even though the possibility of this being an indirect effect can not be ruled out, it is interesting that the same result was not observed when this microarray analysis was applied on a strain deleted of the *TIF4632*, where no accumulation of any pre-mRNA was observed. Our results show that predominantly Tif4631p interacts with spliceosomal U1 snRNP in vitro, and this interaction could be possibly required for efficient processing of certain pre-mRNAs. Analysis and comparison of intron sequences and splice sites of the pre-mRNAs presented in **Table 2** did not reveal any obvious common features between these RNAs, apart from the fact that they are all pre-mRNAs that will give rise to ribosomal proteins. In addition,

five of these RNAs are characterized by the presence of a non-consensus 5' splice site. The interaction of eIF4G with UsnRNPs during splicing in vivo could be possibly necessary as a check point during the processing of these pre-mRNAs. In support of this, a partial but significant co-localization of eIF4G with a proportion of snRNPs at discrete foci was reported in mammalian cells,[20] a finding that strengthens the hypothesis that eIF4G might participate in the processing of some pre-mRNAs in the nucleus.

In conclusion, we present here a detailed mapping of the domains of yeast eIF4G required for interaction with components of the spliceosomal machinery. These interactions probably implicate eIF4G in nuclear RNA processing events in *S. cerevisiae*. Even though yeast eIF4G interacts specifically with spliceosomal components, it is not required for splicing of the RNAs tested in vitro, but a small but significant accumulation of pre-mRNAs is observed in a *tif4631*-Δ strain in vivo. A *tif4632*-Δ strain does not exhibit the same effect, a finding that might explain the normal growth phenotype of this strain, in contrast to the slow growth phenotype of *tif4631*-Δ strain reported by Goyer et al.[19] At present we can not explain why the genetic depletion of one of the eIF4G homologues in yeast affects the splicing of a small number of pre-mRNAs that correspond to ribosomal proteins. There is evidence of an auto-regulatory role for alternative splicing coupled NMD in the expression of a number of ribosomal proteins,[42-44] while MIF4G,[17] a domain that is conserved between eIF4G, Upf2p/NMD2p and CBP80 implicates eIF4G and CBP80 in nonsense-mediated decay. One could suggest that eIF4G participates in nuclear RNA processing by linking in some way pre-mRNA splicing with degradation pathways like NMD and acting once more as a scaffold protein that brings important protein components together.

Materials and Methods

Plasmids and *S. cerevisiae* strains. Plasmids pBS-Tif4631 and pBS-Tif4632 were used as templates for coupled in vitro transcription-translation reactions in rabbit reticulocyte lysates to express [^{35}S]-labeled eIF4G proteins. They were constructed by subcloning PCR amplified *TIF4631* and *TIF4632* genomic DNAs respectively into pBS(SK-) (Stratagene) as EcoR1/BamH1 fragments with primers 5'-GGG AAT TCA TGA CAG ACG AAA CTG TCA AC-3' and 5'-CCG GAT CCT TAC TCT TCG TCA TCA CTT TCT-3' for *TIF4631* and 5'-GGG AAT TCA TGA CTG ACC AAA GAG GTC CAC-3' and 5'-CCG GAT CCT TAA TCA CTG TCC CCA TCG TTA-3' for TIF4632. Plasmid pGEX4T-1-Prp11 was used to express GST-Prp11p. The ORF of PRP11 was subcloned as a Sal1/SmaI fragment from pAS2DD-prp11,[34] into pGEX4T-1 XhoI/SmaI restriction sites. To produce plasmids expressing C-terminally truncated versions of Tif4631, pBS-TIF4631 was digested with each of BstBI, StuI, NheI and BlpI to obtain the 1–765, 1–656, 1–592 and 1–266 truncated forms of Tif4631p respectively. To obtain N-terminally truncated versions, a reverse primer 5'-C*TT A*CT CTT CGT CAT CAC TTT CTC CC-3' and the following forward primers were used to amplify by PCR the fragments of TIF4631 referred next to each primer:

Table 1. *S. cerevisiae* strains used in this study

Name	Genotype
TIF4631::TAP	*MATa ade2-101 his3-Δ200 leu2-Δ1 trp1-Δ99 ura3-Δ 99 cir^{0}tif4631-TAP::TRP1*
TIF4632::TAP	*MATa ade2-101 his3-Δ200 leu2-Δ1 trp1-Δ99 ura3-Δ 99 cir^{0}tif4632-TAP::TRP1*
tif4631-Δ	*MATalpha ade2 his3 leu2 trp1 ura3(GAL$^+$) tif4631Δ::HIS3*
tif4632-Δ	*MATalpha ade2 his3 leu2 trp1 ura3(GAL$^+$) tif4632Δ::HIS3*
tif4631-Δ; TIF4632::TAP	*MATa ade2-101 his3-Δ200 leu2-Δ1 trp1-Δ99 ura3-Δ 99 cir^{0}tif4632-TAP::TRP1 tif4631Δ::HIS3*

5'-GGA TCC TAA TAC GAC TCA CTA TAG GAA CAG ACC ACC *ATG* ACA CCA ATT GAA GAT GTC-3' for amino acids 422–952, 5'-GGA TCC TAA TAC GAC TCA CTA TAG GAA CAG ACC ACC *ATG* GGT CCT GAT ATC AAA TAC for amino acids 438–952, 5'-GGA TCC TAA TAC GAC TCA CTA TAG GAA CAG ACC ACC *ATG* CCA ACT TTC TTG CTT C-3' for amino acids 453–952, 5'-GGA TCC TAA TAC GAC TCA CTA TAG GAA CAG ACC ACC *ATG* GGA GAT TCT GGC AGA TTC GGC-3' for amino acids 494–952, 5'-GGA TCC TAA TAC GAC TCA CTA TAG GAA CAG ACC ACC *ATG* AGA AGA TCA AAG AGA-3' for amino acids 529–952, 5'-GGA TCC TAA TAC GAC TCA CTA TAG GAA CAG ACC ACC *ATG* AAG GAA GAA GTT GCT CC-3' for amino acids 567–952, 5'-GGA TCC TAA TAC GAC TCA CTA TAG GAA CAG ACC ACC *ATG* GAC GGA AAG ACC GAC TAT TGG-3' for amino acids 596–952, 5'-GGA TCC TAA TAC GAC TCA CTA TAG GAA CAG ACC ACC *ATG* GCT ATT GCA AAC ATA TCA G-3' for amino acids 631–952, 5'-GGA TCC TAA TAC GAC TCA CTA TAG GAA CAG ACC ACC *ATG* GCT GTG ATA GAA CAG-3' for amino acids 647–952. The PCR products were purified and used directly in in vitro transcription/translation reactions with rabbit reticulocyte lysates according to manufacturer's instructions (Promega) to obtain the ^{35}S-labeled truncated versions of Tif4631p.

To construct deletion mutant Tif4631p-Δ(565-647), the PCR product produced by forward primer 5'-TAT ACA TAT GGC CCA ACT TTC-3' and reverse primer 5'-CGA CGA TAT CGT CCT CTC TTT TC-3' on pBS-Tif4631 as a template, was digested with NdeI/EcoRV and the PCR product produced by forward primer 5'-CAC CGA TAT CGA ACA GAT TTT C-3' and reverse primer 5'-CGC AGG ATC CAA GAG AAT GAA TGA C-3' was digested with EcoRV/SacII. The digested PCR products were ligated with each other and the pBS-Tif4631 fragment derived from NdeI/SacII digest. For construction of pBS-Tif4631-Δ(504-952), pBS-Tif4631 was digested with MscI/StuI and the respective fragment was gel extracted and ligated.

The strains of *S. cerevisiae* used in this study are described in **Table 1**. Standard yeast growth conditions and manipulations were used.

In situ localization. Yeast strains TIF4631::TAP or TIF463::TAP were grown to OD_{600} = 0.2–0.4 and paraformaldehyde (EMS) was added to final concentration 4%. Cells were harvested, washed in buffer B (1.2 M sorbitol, 65 mM KH_2PO_4, 35 mM K_2HPO_4) at 4°C and resuspended in 1 ml of buffer B.

Table 2. Genes showing a splicing deficiency in the yeast strain *tif4631*-Δ, their respective ORFs and the ratio of pre-mRNA in the *tif4631*-Δ strain compared to the wt strain

Gene	ORF	*tif4631*-Δ/wt	Exon 1	5' splice site	Branch point	3' splice site	Intron size
YBR181C	RPS6B	2.06	gaag	guaugua	uuuacuaacaa	guauuauuuauaacag	352
YOR096W	RPS7A	2.07	agaa	guauguu	cuuacuaacat	uuuccuucuuuuauag	401
YGLI89C	RPS26A	2.22	agua	guauguu	guuacuaacua	augaauauuuaauuag	368
YLR448W	RPL6B	2.33	acaa	guaugug	uauacuaacua	gauaugucaauuauag	384
YHR203C	RPS4B	2.89	gacc	guauguu	uuuacuaacaa	acgauuuuucauauag	269
YJR145C	RPS4A	3.16	gacc	guauguu	uuuacuaacga	auuuuuuuccguacag	256

Sequences of the 5' splice site, the branch point and the 3' splice sites, as well as the size of the corresponding introns are shown (according to Lopez et al.[51]).

After incubation with 1 mg oxalyticase for 10 min at 30°C, cells were washed with ice-cold buffer B and resuspended in 0.65 ml of the same buffer. A 0.1 ml aliquot was put on to a coverslip, allowed to stand for 30 min and then washed with 3 ml of buffer B, replaced with 5 ml of methanol and left for 5 min at -20°C. After a final wash with buffer B, cells were permeabilized by buffer C (0.1% Triton X-100, 20 mM HEPES pH 7.9, 200 mM NaCl) for 30 min. Primary antibody (Rabbit IgG Alexa 488 labelled, Molecular Probes) was used in 1:100 dilution in buffer C, for 1 hr. Washes with buffer C followed and after briefly rinsing with PBS the coverslip was mounted with vectashield with DAPI and examined using a Leica confocal microscope with three lasers giving excitation lines at 380, 488 and 543 nm. The data from the channels were collected separately using narrow-bandpass filter settings. In multiple staining experiments, the laser intensities and data collection settings were adjusted to avoid overlap (bleedthrough) between channels. The coupled microscope was a Leica DMIBRE equipped with a 633 water immersion objective lens (numerical aperture, 1.4). Data sets were processed using the Leica TCS NT, version 1.4.338, software package and were subsequently exported into Adobe Photoshop version 5.5, and Deneba Canvas version 7.02.

In vitro pull down. For purification of GST fusion proteins, *Escherichia coli* extracts from BL21-codon plus cells expressing either GST-Prp11p or GST-Snu71p fusion proteins were prepared by inducing 1 liter culture of exponentially growing cells at OD_{600} of 0.6–0.8, for 3.5 hrs with 1 mM IPTG. Cells were harvested, resuspended in PBS with 0.5% Triton X-100 and lysed by French press. The lysate was incubated with 500 µl of Glutathione-Sepharose beads for 2 hrs at 4°C. The beads were washed extensively with PBS-0.5% Triton X-100 and used subsequently in the binding assays. For in vitro transcription/translation reactions of *TIF4631* or *TIF4632*, the TNT® system (Promega) and plasmids pBS-TIF4631 or pBS-TIF4632 were used according to manufacturer's instructions. For binding assays, GST-fusion proteins bound to glutathione-sepharose beads were incubated with Tif4631p or Tif4632p produced with the TNT® system and the reaction mixtures were incubated for 2 hrs at 4°C. After extensive washing with PBS-0.5% Triton X-100, the proteins were eluted by SDS sample buffer and analysed by SDS/PAGE. For the detection of ^{35}S proteins, the EA starter kit was used (Thistle Scientific).

Purification of Tif4631p-TAP, Tif4632p-TAP proteins. Yeast strains TIF4631::TAP and TIF4632::TAP were grown to OD_{600} = 2 and cells were harvested and lysed in buffer A (10 mM HEPES pH 7.9, 10 mM KCl, 1.5 mM $MgCl_2$, 0.5 mM DTT, 0.5 mM PMSF, 1 µM leupeptin, 2 µM pepstatin A, 4 µM chymostatin, 2.6 µM aprotinin) by French press. The TAP-tagged proteins were purified by incubating the yeast cell lysates with 50 µl of a 50% solution of IgG Sepharose beads for 2.5 hrs at 4°C. To analyse the RNAs that are pulled down by Tif4631-TAP or Tif4632-TAP proteins, the beads were washed extensively with either IPP150 buffer (150 mM NaCl, 0.1% Nonidet P-40, 10 mM Tris, pH 8.0) or IPP350 buffer (350 mM NaCl, 0.1% Nonidet P-40, 10 mM Tris, pH 8.0) and then the RNA was extracted by phenol/chloroform, precipitated and analysed on a 6% acrylamide gel. Northern hybridization followed using the following specific oligonucleotide probes: 5'-CTT AAG GTA AGT AT-3' for U1, 5'-CTA CAC TTG ATC TAA GCC AAA AGG C-3' for U2, 5'-AAT ATG GCA AGC CC-3' for U5, 5'-CTC TTT GTA AAA CGG TTC-3' for U6 and 5'-CCG TGC ATA AGG AT-3' for U4snRNA.

Preparation of whole cell extracts of yeast. The protocol of Umen and Guthrie[45] was used with minor modifications. Namely, the yeast strain of interest was grown to OD_{600} = 0.5–1 at 30°C in 1L YPD medium. Cells were harvested by centrifugation at 5,000 rpm for 5 min (Beckman JLA10.500 rotor) and washed twice with 20 ml of AGK buffer (10 mM HEPES pH 7.9, 1.5 mM $MgCl_2$, 200 mM KCl, 10% Glycerol, 2 mM DTT). Cells were resuspended in 0.4 cell pellet volume of AGK buffer and squirted through a syringe into liquid nitrogen. The frozen cell pellet was ground to a fine powder by mortar and pestle and allowed to thaw. The thawed powder was centrifuged at 17,000 rpm for 30 min at 2°C (rotor JA25.50 Beckman). The supernatant was centrifuged at 40,000 rpm for 1 hr at 4°C (rotor 70.1Ti, Beckman) and subsequently dialysed for 3 hrs against buffer D (20 mM HEPES pH 7.0, 50 mM KCl, 0.2 mM EDTA, 20% (v/v) glycerol) at 4°C, centrifuged at 13,000 rpm for 10 min and frozen at -80°C.

In vitro splicing. In vitro splicing reactions were carried out and analysed as described by Lin et al.[46] Actin pre-mRNA was transcribed from linearized by BamHI plasmid p283,[47] which contains an AluI fragment of the yeast actin gene cloned at a SmaI site of pGEM vector.

Microarrays. Total RNA was prepared as described by Schmitt et al.[48] while the microarrays used were similar to those described by Clark et al.[49] More precisely, there were at least four

oligonucleotide probes per *S. cerevisiae* transcript, containing an intron, immobilized on to the microarray. One probe was complementary to the 5'exon-intron junction of all the pre-mRNAs, one probe was complementary to sequences of the intron, another probe was complementary to the exon-exon junction of all the mature mRNAs and finally there was also a probe that would hybridize to the 3' exon of all the pre-mRNAs and mRNAs used for normalization. For transcripts containing more than one intron and/or different predictions of intron start and end points, the 5' and mature exon-exon junction probes (and occasionally the intron probe) were duplicated as necessary to identify all possible introns. These probes were synthesized by MWG-Biotech AG and have an average length of 41.2 nucleotides. Ideally a probe should have a Tm of 80–90°C (nearest neighbor algorithm), where constraints of the target sequence would allow. Similarly all the probes to a transcript were designed to have a Tm within ±2°C of each other where possible. These probes were printed in triplicate on to poly-lysine slides (Sigma) in 3x SSC buffer at the GTI (Chancellor's Building, Royal Infirmary, Edinburgh) using a GMS 417 (Affymetrix) printer. This microarray was hybridized with Cy dye labeled cDNA derived from total RNA from the mutant strain of interest and an isogenic wild type. The reverse transcription reaction was performed in the presence of Cy dye modified dUTP (Amersham). Either Cy3 or Cy5 was used to label the mutant and the other to label the wild type cDNA, including at least one occasion where the dyes were swapped from their normal total RNA type (dye flip labeling). Thermoscript (Invitrogen) was used to perform the reverse transcription reaction at 47°C using the manufacturer's supplied buffers and 20–50 μg of total RNA. Priming was from gene specific primers designed to bind downstream to the 3' exon probe (45 μM total concentration). The RNA was removed using 55 mM NaOH, 28 mM EDTA pH 8 and 65°C for 30 minutes before neutralization with 120 mM Tris pH 7.5 at 4°C. The labeled cDNAs (mutant and wild type), were combined and spun in YM-100 columns (Millipore), using the manufacturer's instructions, in 10 mM Tris pH 7.5 (used to wash twice more) to filter-purify and concentrate. The arrays were blocked with 1-methyl-2-pyrrolidinone (93% v/v) and succinic anhydride (1.64% w/v) in 68.5 mM boric acid (pH 7 with NaOH) at room temperature for 20 minutes and then pre-hybridized by 5x SSC, 0.1% (w/v) SDS, 1% (w/v) BSA at 47°C for 45 minutes before hybridization. The hybridization solution was 5x SSC, 0.4% (w/v) SDS and 20 μg of human COT-1 DNA in 16 μl under a 22 x 22 mm coverslip at 47°C for 10–16 hrs in a humid chamber. Then the arrays were washed in 1x SSC, 0.2% SDS followed by 0.1x SSC, 0.2% SDS and finally 0.1x SSC, all at room temperature for 5 minutes. Scanning was performed in an Affymetrix 418 scanner and spot quantitation was carried out by ImageQuant v3.1.

To normalize, the background corrected intensity value for each spot was divided by the background corrected intensity value from the corresponding 3'exon probe. More precisely, in a mutant strain where the pre-mRNA of a specific gene is more than the respective mRNA, one would see more RNA hybridized to the oligonucleotides that complement the 5'exon-intron junction or/and intron rather than the one complementary to the exon-exon junction, when compared to the wt strain. The above signals were compared to each other after normalization by the signal the specific RNA gives with the oligonucleotide that hybridizes to each 3' exon and recognizes it in both pre- and mature forms. Additionally, the signal that this RNA gives on the position of the 3'exon recognizing oligonucleotide probe should be equal to the sum of the signal it gives with the 5'exon-intron recognizing oligonucleotide probe, plus the signal from the hybridization with the exon-exon junction recognizing oligonucleotide probe. On the other hand, the same amount of RNA is expected to hybridize to the oligonucleotide probe that complements the 3' exon of this RNA for both control and mutant strain, since the total amount of the specific RNA should be equal in both strains.

For the primer extension experiments performed to check the microarray results, total RNA prepared as described above was hybridized with a ^{32}P-labeled oligonucleotide probe with the sequence 5'-AGA AAG ACA ATC AAT GGC AAG GA-3' that hybridizes in exon 2 of the YJR145C pre-mRNA. The reverse transcription reaction was performed as described by Bousquet-Antonelli et al.[50]

Acknowledgements

We thank Heike Roesner for help with the mapping of eIF4G interaction domains. We thank Skarlatos G. Dedos, and Tuija A.A. Pöyry for critical reading and comments on the manuscript. We also thank Prof. Richard J. Jackson (Dept. of Biochemistry, University of Cambridge) for his support. Research in the laboratory of J.L. was initially supported by the Medical Research Council. E.T. and A.J. were funded by the RNOMICS project QLG2-CT-2001-01554. J.D.B. was funded by the Wellcome Trust grant 067311 to Prof. Jean Beggs. P.K. held a Marie-Curie Fellowship (R81517).

References

1. Izaurralde E, Lewis J, McGuigan C, Jankowska M, Darzynkiewicz E, Mattaj IW. A nuclear cap binding protein complex involved in pre-mRNA splicing. Cell 1994; 78:657-68.
2. Lewis JD, Gorlich D, Mattaj IW. A yeast cap binding protein complex (yCBC) acts at an early step in pre-mRNA splicing. Nucleic Acids Res 1996; 24:3332-6.
3. Flaherty SM, Fortes P, Izaurralde E, Mattaj IW, Gilmartin GM. Participation of the nuclear cap binding complex in pre-mRNA 3' processing. Proc Natl Acad Sci USA 1997; 94:11893-8.
4. Gorlich D, Kraft R, Kostka S, Vogel F, Hartmann E, Laskey RA, et al. Importin provides a link between nuclear protein import and U snRNA export. Cell 1996; 87:21-32.
5. Visa N, Izaurralde E, Ferreira J, Daneholt B, Mattaj IW. A nuclear cap-binding complex binds Balbiani ring pre-mRNA cotranscriptionally and accompanies the ribonucleoprotein particle during nuclear export. J Cell Biol 1996; 133:5-14.
6. Shen EC, Stage-Zimmermann T, Chui P, Silver PA. The yeast mRNA-binding protein Npl3p interacts with the cap-binding complex. J Biol Chem 2000; 275:23718-24.
7. Furuichi Y, LaFiandra A, Shatkin AJ. 5'-Terminal structure and mRNA stability. Nature 1977; 266:235-9.
8. Shatkin AJ. mRNA cap binding proteins: Essential factors for initiating translation. Cell 1985; 40:223-4.
9. Ohno M, Kataoka N, Shimura Y. A nuclear cap binding protein from HeLa cells. Nucleic Acids Res 1990; 18:6989-95.
10. Colot HV, Stutz F, Rosbash M. The yeast splicing factor Mud13p is a commitment complex component and corresponds to CBP20, the small subunit of the nuclear cap-binding complex. Genes and Dev 1996; 10:1699-708.
11. Mazza C, Segref A, Mattaj IW, Cusack S. Large-scale induced fit recognition of an m(7)GpppG cap analogue by the human nuclear cap-binding complex. EMBO J 2002; 21:5548-57.
12. Lewis JD, Izaurralde E, Jarmolowski A, McGuigan C, Mattaj IW. A nuclear cap-binding complex facilitates association of U1 snRNP with the cap-proximal 5' splice site. Genes Dev 1996; 10:1683-98.

13. Fortes P, Kufel J, Fornerod M, Polycarpou-Schwarz M, Lafontaine D, Tollervey D, Mattaj IW. Genetic and physical interactions involving the yeast nuclear cap-binding complex. Mol Cell Biol 1999; 19:6543-53.
14. Gingras AC, Raught B, Sonenberg N. eIF4 initiation factors: effectors of mRNA recruitment to ribosomes and regulators of translation. Annu Rev Biochem 1999; 68:913-63.
15. Dominguez D, Kislig E, Altmann M, Trachsel H. Structural and functional similarities between the central eukaryotic initiation factor (eIF)4A-binding domain of mammalian eIF4G and the eIF4A-binding domain of yeast eIF4G. Biochem J 2001; 355:223-30.
16. Hentze M. eIF4G: a multipurpose ribosome adapter. Science 1998; 275:500-1.
17. Ponting CP. Novel eIF4G domain homologues linking mRNA translation with nonsense-mediated mRNA decay. Trends Biochem Sci 2000; 25:423-6.
18. Aravind L, Koonin EV. Eukaryote-specific domains in translation initiation factors: implications for translation regulation and evolution of the translation system. Genome Res 2000; 10:1172-84.
19. Goyer C, Altmann M, Lee HS, Blanc A, Deshmukh M, Woolford JL Jr, et al. TIF4631 and TIF4632: Two yeast genes encoding the high-molecular-weight subunits of the cap-binding protein complex (eukaryotic initiation factor 4F) contain an RNA recognition motif-like sequence and carry out an essential function. Mol Cell Biol 1993; 13:4860-74.
20. McKendrick L, Thompson E, Ferreira J, Morley SJ, Lewis JD. Interaction of eukaryotic translation initiation factor 4G with the nuclear cap-binding complex provides a link between nuclear and cytoplasmic functions of the m(7)guanosine cap. Mol Cell Biol 2001; 21:3632-41.
21. Lejeune F, Ranganathan AC, Maquat LE. eIF4G is required for the pioneer round of translation in mammalian cells. Nat Struct Mol Biol 2004; 11:992-1000.
22. Ishigaki Y, Li X, Serin G, Maquat LE. Evidence for a pioneer round of mRNA translation: mRNAs subject to nonsense-mediated decay in mammalian cells are bound by CBP80 and CBP20. Cell 2001; 106:607-17.
23. Lejeune F, Ishigaki E, Li X, Maquat LE. The exon junction complex is detected on CBP80-bound but not eIF4E-bound mRNA in mammalian cells: Dynamics of mRNP remodeling. EMBO J 2002; 21:3536-45.
24. Hentze MW, Kulozik AE. A perfect message: RNA surveillance and nonsense-mediated decay. Cell 1999; 96:307-10.
25. Maquat LE, Carmichael GG. Quality control of mRNA function. Cell 2001; 104:173-6.
26. Schell T, Kulozik AE, Hentze MW. Integration of splicing, transport and translation to achieve mRNA quality control by the nonsense-mediated decay pathway. Genome Biol Reviews 2002; 3:1006.
27. Maquat LE. Nonsense-mediated mRNA decay in mammals. J Cell Science 2005; 118:1773-6.
28. Ferraiuolo MA, Lee C-S, Lian LW, Hsu JL, Costa-Mattioli M, Luo M-J, et al. A nuclear translation-like factor eIF4AIII is recruited to the mRNA during splicing and functions in nonsense-mediated decay. PNAS 2004; 101:4118-23.
29. Fortes P, Inada T, Preiss T, Hentze M, Mattaj IW, Sachs AB. The yeast nuclear cap binding complex can interact with translation factor eIF4G and mediate translation initiation. Mol Cell 2000; 6:191-6.
30. Iborra FJ, Jackson DA, Cook PR. Coupled transcription and translation within nuclei of mammalian cells. Science 2001; 293:1139-42.
31. Dahlberg JE, Lund E, Goodwin EB. Nuclear translation: What is the evidence? RNA 2003; 9:1-8.
32. Nathanson L, Xia T, Deutscher MP. Nuclear protein synthesis: A reevaluation. RNA 2003; 9:9-13.
33. Baron-Benhamou J, Fortes P, Inada T, Preiss T, Hentze MW. The interaction of the cap-binding complex (CBC) with eIF4G is dispensable for translation in yeast. RNA 2003; 9:654-62.
34. Fromont-Racine M, Rain J-C, Legrain P. Towards a functional analysis of the yeast genome through exhaustive two-hybrid screens. Nat Genetics 1997; 16:277-82.
35. Ho Y, Gruhler A, Heilbut A, Bader GD, Moore L, Adams SL, et al. Systematic identification of protein complexes in *Saccharomyces cerevisiae* by mass spectrometry. Nature 2002; 415:180-3.
36. Tarun SZ Jr, Sachs AB. Association of the yeast poly(A)-tail binding protein with translation initiation factor eIF-4G. EMBO J 1996; 15:7168-77.
37. Mader S, Lee H, Pause A, Sonenberg N. The translation initiation factor eIF-4E binds to a common motif shared by the translation factor eIF-4gamma and the translational repressors 4E-binding proteins. Mol Cell Biol 1995; 15:4990-7.
38. Barrass JD, Beggs JD. Splicing goes global. Trends Genet 2003; 19:295-8.
39. Etchison D, Etchison JR. Monoclonal antibody-aided characterization of cellular p220 in uninfected and poliovirus-infected HeLa cells: subcellular distribution and identification of conformers. J Virol 1987; 61:2702-10.
40. Huh W-K, Falvo JV, Gerke LC, Carroll AS, Howson RW, Weissman JS, O'Shea EK. Global analysis of protein localization in budding yeast. Nature 2003; 425:686-91.
41. Stevens SW, Ryan DE, Ge HY, Moore RE, Young MK, Lee TD, Abelson J. Composition and functional characterization of the yeast spliceosomal penta-snRNP. Mol Cell 2002; 9:31-44.
42. Cuccurese M, Russo G, Russo A, Pietropaolo C. Alternative splicing and nonsense-mediated mRNA decay regulate mammalian ribosomal gene expression. Nucleic Acids Res 2005; 33:5965-77.
43. Dabeva MD, Warner JR. Ribosomal protein L32 of *Saccharomyces cerevisiae* regulates both splicing and translation of its own transcript. J Biol Chem 1993; 268:19669-74.
44. Mitrovich QM, Anderson P. Unproductively spliced ribosomal protein mRNAs are natural targets of mRNA surveillance in *C. elegans*. Genes Dev 2000; 14:2173-84.
45. Umen JG, Guthrie C. Mutagenesis of the yeast gene PRP8 reveals domains governing the specificity and fidelity of 3' splice site selection. Genetics 1996; 143:723-39.
46. Lin R-J, Newman AJ, Cheng S-C, Abelson J. Yeast mRNA splicing in vitro. J Biol Chem 1985; 260:14780-92.
47. O'Keefe RT, Norman C, Newman AJ. The invariant U5 snRNA loop 1 sequence is dispensable for the first catalytic step of pre-mRNA splicing in yeast. Cell 1996; 86:679-89.
48. Schmitt ME, Brown TA, Trumpower BL. A rapid and simple method for preparation of RNA from *Saccharomyces cerevisiae*. Nucl Acids Res 1990; 18:3091-2.
49. Clark TA, Sugnet CW, Ares M Jr. Genomewide analysis of mRNA processing in yeast using splicing-specific microarrays. Science 2002; 296:907-10.
50. Bousquet-Antonelli C, Presutti C, Tollervey D. Identification of a regulated pathway for nuclear pre-mRNA turnover. Cell 2000; 102:765-75.
51. Lopez PJ, Séraphin B. YIBD: the Yeast Intron DataBase. Nucleic Acids Res 2000; 28:85-6.